ENG. Struct. Civ. Eng. 2026, 20(4): 657–673
https://doi.org/10.1007/s11709-026-1311-y

RESEARCH ARTICLE

Effects of soluble soybean polysaccharide on the distribution of biomineral precipitation in aeolian sands: Experiments and numerical analysis

Yunqi GAO[a,b], Zichuang ZHANG[a,b], Liya WANG[c*], Yongshuai QI[d], Haiqing ZHANG[a,b], Yufeng GAO[e], Leon van PAASSEN[f]

[a] *College of Civil Engineering and Architecture, Hebei University, Baoding 071002, China*
[b] *Hebei Key Laboratory of Infrastructure Disaster Mitigation and Intelligent Assessment, Baoding 071002, China*
[c] *Key Laboratory of Roads and Railway Engineering Safety Control (Shijiazhuang Tiedao University), Ministry of Education, Shijiazhuang 050043, China*
[d] *Academy of Combat Support, Rocket Force University of Engineering, Xi'an 710025, China*
[e] *Key Laboratory of Ministry of Education for Geomechanics and Embankment Engineering, Hohai University, Nanjing 210098, China*
[f] *School of Sustainable Engineering and the Built Environment, Arizona State University, Tempe, AZ 85281, USA*
[*] *Corresponding author. E-mail: lwang@stdu.edu.cn*

ABSTRACT The biologically induced precipitation method has demonstrated great potential in enhancing the wind erosion resistance of desert aeolian sands due to its low-cost and sustainability. This method, however, often results in unevenly biomineral distribution, leading to suboptimal performance despite consistent precipitation content. This study explored soluble soybean polysaccharide (SSPS) as a natural additive to improve the spatial distribution of biominerals in aeolian sands treated by soybean-urease induced carbonate precipitation (SICP). A series of liquid batch tests and soil column experiments were conducted. The overall reaction rate was quantified using ammonium production data and modeled using first-order kinetics. The results show that incorporation of 3 g/L SSPS improves the uniformity of biomineral distribution, which reduced the largest deviation from 44% to 2% without reducing the reaction rate. On the contrary, the reaction rate increases by 1.5 times compared to the case without SSPS. Numerical analysis and protein measurements indicate that SSPS improves the uniformity of urease distribution. The dual enhancement in the uniformity of biomineral distribution and reaction rate can be attributed to the protein-stabilizing properties of SSPS, which can mitigate enzyme flocculation and sustain catalytic capacity throughout the soil column. The dual optimizing effects make SSPS a promising and effective bio-compatible additive for improving the efficiency of SICP in porous media.

KEYWORDS SICP, SSPS, calcium carbonate distribution, experimental-numerical approach, porous media

1 Introduction

Land desertification has become a global ecological crisis that poses a significant threat to human security. The International Union for Conservation of Nature and Natural Resources estimated a loss of about 6.3 to 10.6 trillion dollars annually for global loss of ecosystem services due to land degradation and desertification. Many attempts have been applied to mitigation of sandstorms and controlling desertification including the mechanical barriers that slow down the wind speed and block wind blowing aeolian sands, organic polymer materials covering that increase the erosion resistance of the surficial soils and biological method that induce microorganisms to amelioration aeolian sands.

Biologically induced precipitation techniques have emerged as a promising approach to combat desertification [1–5]. Among the biologically induced techniques,

Article history: Received Oct 28, 2025; Accepted Jan 13, 2026

urea hydrolysis is one of the most widely studied processes, where microbes or free urease enzymes catalyze the hydrolysis of urea to produce carbonate and hydroxide. In the presence of calcium, carbonate reacts in the alkaline environment to form calcium carbonate precipitates. This process is termed microbially induced carbonate precipitation (MICP) or enzymatically induced carbonate precipitation (EICP), depending on whether microbes or free enzymes are used as the functional medium. The overall reaction can be expressed by a combined equation, as shown in Eq. (1). EICP and MICP have distinct advantages and applications. Due to the smaller size of free enzymes compared to microbes, EICP is more suitable for treating fine-grained soils. Gao et al. investigated the possibility of cementing silty soil by EICP using soybean extracted urease [6]. The results indicated that silty samples were not clogged even with 15 treatments. In contrast, MICP may result in higher carbonate precipitation content under certain conditions [7]. Xiao et al. [8] proposed a two-stage degradation mechanism and a thermodynamic constitutive model for dynamic liquefaction of microbial-cemented calcareous sand under cyclic loading. Their work revealed the fundamental principles of the liquefaction resistance of MICP-treated sand, providing a robust theoretical analytical method for simulating the dynamic characteristics of microbially reinforced soils. Free urease is commercially available [9–11] or can be extracted from ureolytic bacteria cultures [12–16] and various plant sources, including soybean [17–19]. Considering the high cost of commercial urease, crude urease extracted from soybean is widely used in many studies. It is typically prepared by soaking soybean powder in water, followed by filtration or further purification to varying degrees. The method of inducing calcium carbonate precipitation using soybean urease is referred to as the SICP (Soybean-urease Induced Carbonate Precipitation) method.

$$\mathrm{CO(NH_2)_2(aq) + 2H_2O(l) + Ca^{2+}(aq) \xrightarrow{urease} CaCO_3(s) + 2NH_4^+(aq)} \quad (1)$$

Expanding on the SICP framework, urease, along with urea and calcium solutions, is sprayed onto or flushed into aeolian soil to bind particles and densify the soil, thereby improving its resistance to wind erosion [4,20]. Treatment uniformity is one of the concerns when applying SICP to improve the performance of soils, especially for fine soils [21–24]. Neupane et al. [25] and Nafisi et al. [23] mentioned that uniformity of the distribution of calcium carbonate precipitation ($CaCO_3$) affects the efficiency of strength improvement in biologically treated soils. Lots of efforts are made to optimize the treatment procedure aiming at improving the uniformity of the treated soil to get higher strength with low precipitation content or less substrate inputs.

Normally two strategies were adopted to innervate the distribution of $CaCO_3$: one is lowering the reaction rate, which enables substrates migrate further from the inlet, and the produced carbonate can precipitation with transported calcium at deeper locations; the other is improving the urease transportation along the soil by weakening the surface clogging, reducing flocculation of enzymes, improving absorbance or combined techniques to get a more uniform distribution of urease. Neupane et al. [25] observed that with one pore volume of flush under a constant head, substrates without enzyme distributed almost evenly along the soil column but not the biominerals. The distribution of calcium carbonate is mainly influenced by the distribution of enzymes at the same condition. Based on simulated fracture mineralization deposition experiments, Zhao et al. [26] elucidated the mechanisms by which high concentrations of urease promote the deposition of amorphous products and high concentrations of cementation solution inhibit deposition. They proposed a homogeneity index of deposition distribution and identified high reaction rates as the primary cause of the heterogeneity in calcium carbonate deposition distribution. Cui et al. [21] adopted a one-phase low-pH (pH = 6.5) technique to cement clean Ottawa 20–30 sand and observed a more uniform biomineral distribution and high unconfined compressive strength (UCS) in SICP treated soil. The uniform biomineral distribution is due to the low reaction rate caused by the low pH, which provides adequate time for transportation of the treatment solution into soils before precipitation occurrence. On the other hand, Cheng et al. [27] pointed out that with low-pH, the immediate bio-flocculation in treatment solution was also overcome so that the enzyme clogging at the inlet of specimen could be reduced. It should be mentioned that the low reaction rate requires more time and maybe more input to get the target precipitation contents, considering the low stability of free enzymes. Yan et al. [28] used some strong electrolytes ($CaCl_2$ and $MgCl_2$) to reduce the excess protein in the crude extracted urease by salting out, which depresses the clogging effects and improves the uniformity of urease. However, the urease activity was also diminished together with the reduction of proteins in the salting-out technique and the low-pH technique. Meanwhile, the extra step of the salting out process also consumes resources.

Additives can be used to mitigate the problem of uneven enzyme distribution by reducing the tendency of enzymes aggregation. Soluble soybean polysaccharide (SSPS), a water-soluble polysaccharide extracted from soybean residue, normally serves as a dispersing agent and stabilizer in the food industry. It prevents proteins aggregation without increasing viscosity, making it a potential compound to improve enzyme distribution in SICP. Meanwhile, SSPS is reported to protect protein

from denaturation under low temperature [29] and also to promote the acidifying activity of probiotic [30]. The function of suppressing protein aggregation and protection may influence the distribution of urease in a porous medium. However, for SICP the effects of SSPS on the activity and distribution of crude extracted soybean urease are unknown yet.

In this study, SSPS was investigated as an additive in the treatment solution to improve the uniformity of calcium carbonate precipitation (biominerals) in SICP-treated soil. The distribution of biominerals in SICP is influenced by various factors, including reaction rate, enzyme flocculation, surface clogging, and enzyme transport. These factors primarily affect uniformity through two mechanisms: the reaction rate, as discussed by Cheng et al. [27], and the distribution of enzymes, as highlighted by Barkouki et al. [31] and Neupane et al. [25]. To examine the effects of SSPS on biomineral distribution, a hybrid experimental-numerical approach was adopted. Liquid environment tests were conducted to evaluate the influence of SSPS on the activity of crude soybean urease and the overall reaction process of SICP. Reaction rates, with and without SSPS, were determined from batch test results. Additionally, a one-dimensional transport-reaction model was employed to simulate biomineral formation and distribution, incorporating porosity reduction and permeability changes. Soil column tests were performed to measure calcium carbonate precipitation at different column depths (top, middle, and bottom). The simulation results were compared with experimental data to validate the model and analyze the enzyme distribution.

2 Methodology

As mentioned above, the optimization of calcium carbonate precipitation distribution induced by SICP in soils through the addition of SSPS can be theoretically attributed to the alteration of urease activity and the improvement of enzyme distribution. To investigate these effects, a series of urease activity tests, liquid batch tests, and soil column tests were conducted in this study. Under aqueous conditions, urease activity was measured through conductivity change of urea solution (without addition of calcium) during the initial phases of urea hydrolysis, both with and without the addition of 3 g of SSPS, to evaluate its influence on enzymatic performance. Liquid batch tests were further performed to examine the impact of SSPS on the whole SICP process, including urea hydrolysis and subsequent carbonate precipitation. Since SSPS may also affect the transport characteristics of enzymes and substrates along the soil, resulting in different enzyme distribution, soil column tests were conducted to evaluate the combined effects of SSPS on SICP reaction and enzyme distribution. The final biomineral distribution along the soil column was then measured to assess these combined effects.

2.1 Urease activity and liquid batch test

The soybean urease used in this study was crude enzyme extracted from 60 g/L soybean solution. Dried soybeans (60 g) were grinded and soaked in deionized water for 30 min. The mixture was homogenized using a magnetic stirrer, followed by filtration through a gauze. The filtrate was centrifuged for 15 min, and the supernatant of the suspension was further filtered using a 200-mesh gauze to obtain the crude enzyme solution.

To determine the urease activity, 3 mL extracted enzyme solution was added to 27 mL of 1.11 mol/L urea solution, resulting in a final urea concentration of 1 mol/L. The activity of urease was tested at 20 °C by measuring conductivity changes over 15 min, following the method of Whiffin [32]. For comparison, 3 g/L of commercially available food-grade SSPS (80% purity) was added to the enzyme solution prior to testing. SSPS properties include 1.4% protein, 8.0% ash, and 5.47% water by weight. Its aqueous solution has a viscosity of 1.3 mPa·s at 20 °C and does not form gels under the tested conditions.

Liquid batch tests were conducted to test the effects of SSPS on SICP reaction process. The cementing solution contained urease, urea and calcium chloride, prepared at specific concentrations and mixed at a 1:1 volume ratio. Urease extracted from 60 g soybean, with or without 3 g/L SSPS, was then added to the cementing solution at a 1:1 volume ratio, resulting in initial urea and calcium concentration of 0.4 mol/L. As urea was hydrolyzed by urease to ammonium, the concentration of ammonium was periodically measured to monitor the progress of the reaction. Ammonium concentrations were determined using a colorimetric assay, where the intensity of color produced by the reaction with Nessler's reagent was linearly correlated with ammonia nitrogen concentrations within the range of 0–100 μg/L. The color intensity was measured at 420 nm using a spectrophotometer. Calcium concentrations were measured by the EDTA (Ethylenediaminetetraacetic acid) titrimetric method (ISO 6058) [33], as described by Gao et al. [34]. The measured ammonium concentrations were converted to urea concentration according to Eq. (1) to get the reaction rate of the whole SICP process in different cases.

2.2 Soil column tests

The soil columns in this study were made by aeolian sands collected from the south-east edge of the Tengger Desert. The main component of the soil is quartz (silicon dioxide). The grain size of the aeolian sand ranges from

0.075 to 0.25 mm with a mean grain size of approximately 0.164 mm, and the grain-size distribution curve of aeolian sands is shown in Fig. 1. The coefficients of uniformity and curvature are 1.413 and 1.055, respectively. The specific gravity is 2.66, and the maximum and minimum dry density of the aeolian sands are 1.72 and 1.44 g/cm^3, respectively. According to ASTM D2487-00, the soil is classified as poorly graded sand [35].

To prepare the soil columns, 300 g of dry aeolian sand were placed by five layers into a split-acrylic-cylindrical mold. A 300-mesh screen was placed at the bottom of the specimen to prevent leakage of sand particles. The height of the specimens was 100 mm, and the diameter was 50 mm. The bulk dry density of the specimen was 1528 kg/m^3 and the porosity was 0.425, which corresponds to a relative density of about 35.3%. Cementation solutions were flushed into the soil column with open ends for treatment. A large-pore mesh was placed at the flat top of the soil specimen to minimum the interruption during treatment. Cementation solutions were prepared by mixing equal volume of crude soybean enzyme solution and cementation solution, which contained equimolar of urea and calcium chloride. The resulting concentration of urea and calcium in the cementation solution was 0.4 mol/L. A total of 90 mL of the treatment solution, with or without 3 g/L SSPS, was flushed through the specimen. The bottom of the specimen was kept open during flushing to allow proper drainage.

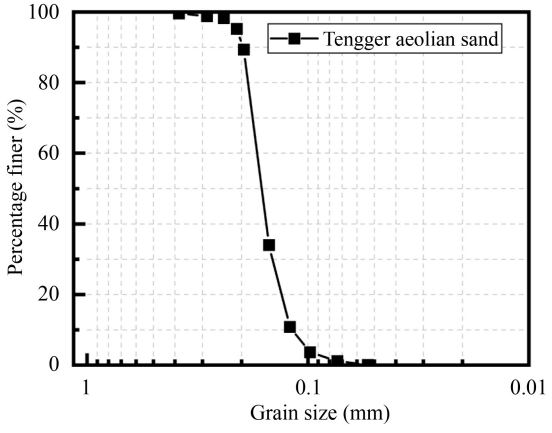

Fig. 1 Grain-size distribution curve of aeolian sands.

The tests were conducted three times for each condition to ensure reproducibility. The initial intrinsic permeability of the soil before treatment was determined by the constant-head permeability test, yielding a value of 2.528×10^{-11} m^2. The flushing process took approximately 12 min for 90 mL of solutions to pass through the specimen. After flushing, the residual solution was left in the specimen for 30 h to allow the reaction to proceed.

After reaction, samples were collected from the top, middle, and bottom of these specimens to determine the calcium carbonate contents. Each sample was acid-digested, and calcium concentration was determined using the EDTA titration method (ISO 6058) [33], as described by Gao et al. [34]. The calcium carbonate content was calculated based on the volume of acid used and the measured calcium concentration and was expressed as a percentage of the dry soil mass. Figure 2 shows the schematic diagram of experimental procedures.

3 Results

3.1 Urease activity and liquid batch test

The activity of extracted urease used in this study was

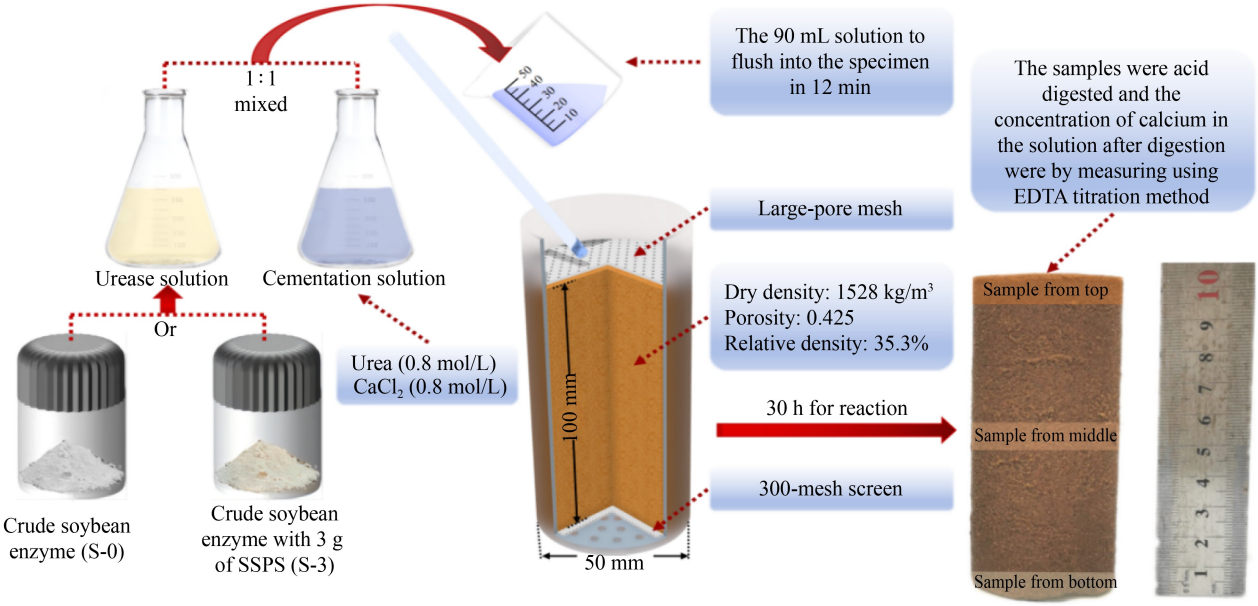

Fig. 2 Schematic diagram of experimental procedures.

11.38 and 11.26 mmol urea per minute per liter with 3 g/L SSPS addition. The minimal difference in these values indicates that SSPS has negligible effects on the extracted crude soybean urease activity. The temporal evolution of ammonium ($NH4^+$) and calcium (Ca^{2+}) concentrations in the liquid batch tests, with and without SSPS, is presented in Fig. 3. The concentration developments of ammonium and calcium with time can be divided into four stages. Stage I refers the initial reaction phase for the first 0.25 h. During this stage, urea was hydrolyzed at nearly the identical rate in both the S-0 (no SSPS) and S-3 (with 3 g/L SSPS) conditions, but the concentration of calcium remained almost unchanged. The similar reaction rate increased the ammonium concentration from 0 to 0.077 mol/L in both cases, which means that initially, the addition of 3 g of SSPS has little effect on the reaction rate. After the first stage, the ammonium concentration gradually increased to 0.146 mol/L for S-0 and 0.171 mol/L for S-3 at 1 h. The converted ammonium is a bit higher in S-3 than that in S-0, which indicates that the catalytic efficiency of urease is increased a bit by the addition of 3 g/L SSPS. On the other hand, there were barely calcium concentration changes in both cases. The maximum calcium concentration drop was only 0.03 mol/L happened in S-0 during 0.75 to 1 h. The delay between carbonate production and calcium carbonate precipitation is due to the requirement of calcium carbonate supersaturation and nucleation for biomineral precipitation [36–38].

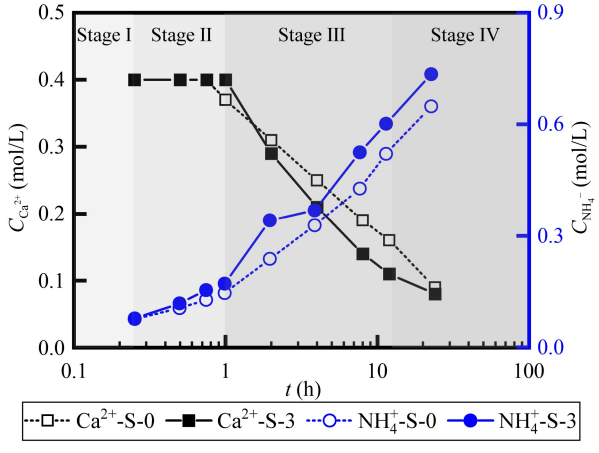

Fig. 3 Developments of ammonium and calcium concentration in the liquid batch tests.

In Stage III, which started from the 1st to the 8th h, the produced ammonium in S-3 was much more than that in S-0. The ammonium concentration reached 0.525 mol/L for S-3, which was 22.7% higher than that in S-0 (0.428 mol/L) after 8 h of reaction. The positive effect of SSPS on the reaction rate increased during this period compared to Stage II. Meanwhile, the concentration of calcium decreased sharply due to the production of massive carbonate and hydroxide. The decreasing rate of calcium concentration was also much higher in S-3 compared to S-0. The residual calcium concentration was 0.14 mol/L for S-3, 26.3% lower than that for S-0, which was about 0.19 mol/L. Later on, the reaction went to Stage IV, in which the two development curves of ammonium concentration were parallel after 8 h of reaction as shown in Fig. 3. It indicates that the rate of urea hydrolysis was almost the same in both cases, with the final ammonium concentration of 0.648 and 0.735 mol/L for S-0 and S-3, respectively. The ammonium centration at the end of the test is a bit higher for S-3 than that for S-0, exhibiting a larger conversion efficiency of urea. For calcium, the decreasing rate goes down a little bit for S-3 after 12 h and finally reaches almost a similar value at about 0.1 mol/L for both cases though it was a bit lower for S-3.

The consuming rate of urea is controlled by the total catalytic rate of the extracted enzymes, which should be related to the amount of active enzyme protein (or more specifically the active sites) and the unit activity of the protein and sites. Given the activity is not so much affected by 3 g/L SSPS as shown in the activity tests, it is reasonable to hypothesis that the active catalytic sites were more for the S-3 condition during Stage II and III. Two possible explanations can be proposed for this phenomenon: 1) a direct increase of catalytic capacity induced by SSPS considering the common botanical source (soybean) of SSPS and urease; 2) an indirect enhancement to the apparent rate of urea hydrolysis due to the mitigation of reaction inhibitors, such as enzyme flocculation. To inspect the first mechanism, 3 mL of 3 g/L SSPS was added to 27 mL of 1.11 mol/L urea solution to measure the conductivity change within 15 min at 20 °C. The results showed that the 3 g/L SSPS solution has negligible activity (0.04 mmol urea /(min·L)) for urea hydrolysis. The extremely weak activity is understandable as SSPS is extracted from Okara, the residue of soybean. Based on the analysis and results, it is reasonable to hypothesis that 3 g/L of SSPS have the function of protecting the active sites of the enzymes.

To quantitively assess the effects of SSPS on SICP reaction, the reaction rates were analyzed based on the concentration developments of urea for S-0 and S-3. The developments of urea concentration, which are obtained based on the ammonium concentration according to Eq. (1) are shown in Fig. 4. Many kinetics were used to describe enzymatic dynamics, including Michaelis-Menten equation, first-order kinetics, second-order kinetics and so on [39–42] compared the first-order, zero-order, first-and zero-order, first-plus linear-order and hyperbolic models to obtain ureolytic reaction rate and found that the first-order kinetic best fit the data [41]. In this study, the first-order rate reaction kinetics with consideration of enzyme concentration is assumed to describe SICP with respect to the concentration of urea.

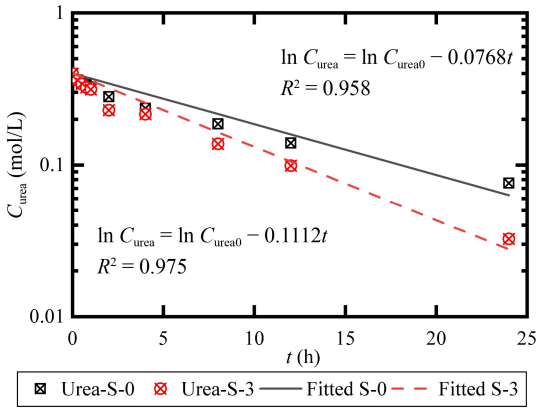

Fig. 4 The converted urea concentration developments and the fitting results of cases with (S-3) and without 3 g/L SSPS addition (S-0).

In the first-order reaction, the reaction rate (R) is linearly related to the concentration of limiting substrate, which is urea in urea hydrolysis as shown in Eq. (2). k_i is the first-order reaction constant. It should be noted that the reaction rate constant k_i represents the value of the whole process in the liquid batch tests and is the produce of catalytic rate of unit enzyme and the enzyme concentration as shown in Eq. (3). One benefit of using the first-order reaction rate is that there's only one parameter (k_i) in the equation and this parameter can be easily obtained based on the development of urea concentration. The theoretical relationship of urea concentration development with time, as shown in Eq. (4), can be obtained by the integrated form of Eq. (2), where C_{urea0} is the initial concentration of urea before reaction. k_i was then linearly fitted based on the experimental results of urea concentration. The fitting results are shown in Fig. 4 as well. k_i are 0.0768 and 0.1112 h^{-1} for S-0 and S-3, respectively. It can be concluded that 3 g of SSPS can increase the reaction rate of SICP by about 1.5 times compared with no SSPS addition.

$$R = -\frac{dC_{urea}}{dt} = k_i C_{urea}, \quad (2)$$

$$k_i = r_i C_e, \quad (3)$$

$$\ln C_{urea} = \ln C_{urea0} - k_i t, \quad (4)$$

where R is the reaction rate, k_i are the first-order reaction rate constants for SICP with or without SSPS addition, while i indicates the concentration of SSPS addition, r_i are the specific uptake rates for unit enzyme, and C_e is the concentration of enzymes, C_{urea} and C_{urea0} are real-time and initial concentration of urea.

It should be noted that, based on the analysis of the activity and liquid batch tests, the initial concentrations of the active enzyme protein are almost the same in S-0 and S-3. However, the catalytic capacities of these enzymes are changed during the reaction, resulting in different reaction rates in these two cases. The changed capacity is due to the changes of active sites. The number of active sites cannot be quantitively identified. However, the active sites can be averagely considered into the specific uptake rates of one malar of total urease protein. For the same amount of urease, the more active site, the higher specific uptake rates. The concentration of total enzymes can be determined based on the mass concentration of enzyme added in the cementation solution and the molar mass of urease enzymes. In the liquid phase, r_i equals k_i/C_{et}, where C_{et} is the total concentration of enzyme and k_i is the total reaction rate which can be determined by the urea developments in the liquid batch tests. Meanwhile, in terms of the reaction happening in the porous medium, the reaction rate at different locations will be different considering heterogeneous distributions of enzymes due to the transportation process. The local reaction rate is related to the local enzymes concentration (C_e) and the specific uptake rates r_i, which can be taken as the same values determined in the liquid phase under different conditions.

3.2 Soil column tests

Calcium carbonate precipitation contents at the top, middle and bottom parts of the sand column after a single SICP treatment with and without 3 g/L SSPS were measured. The measurements were run in triplicate. The results are presented as the percentage of precipitated mass to the dry sand mass as shown in Fig. 5. In the absence of SSPS, there are big differences between the top, middle and bottom of the samples. The largest precipitation contents are observed at the top of the S-0 samples, which is about 0.81%. With increasing distance from the inlet, the precipitation contents decrease fast resulting in only about 0.45% at the bottom. On the contrary, the precipitation contents show a more homogeneous distribution with 3 g/L of SSPS addition.

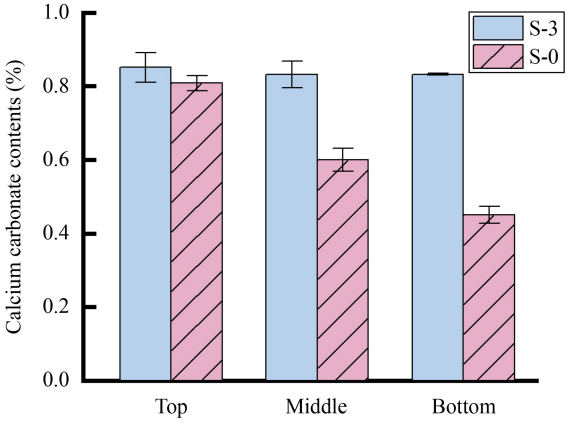

Fig. 5 The calcium carbonate contents at different locations of S-0 and S-3 scenarios.

The top of the sample has 0.85% precipitation while the bottom has 0.83% for S-3.

It is interesting that the precipitation contents show a more homogenous distribution with a bit higher average value for S-3 samples compared to S-0 samples based on the analysis in the liquid environment test. Since the reaction rate of the whole SICP process with 3 g/L of SSPS is about 1.5 times of that without SSPS, it should result in a more uneven precipitation distribution for S-3 when compared with S-0 if similar enzyme distributions are assumed [21,27,43]. However, the actual precipitations distribute heterogeneously in S-0 but homogeneously in S-3. The possible mechanism is due to the different enzyme distribution in S-0 and S-3. In SICP without SSPS addition, the enzymes have been reported to form flocs with calcium cations and the large flocs might clog the pores near the inlet [28]. More enzymes will gather near the inlet and fewer enzymes can penetrate into deeper locations, resulting in heterogeneous enzyme distribution. Meanwhile, the gathered enzymes will produce more calcium carbonate within the same time and, together with the large flocs, extend the retention time of the substrates by reducing porosity and permeability. On the contrary, the enzymes might be more evenly distributed in S-3. The local variability related to these processes is hard to acquire through experiments. Hommel et al. [44] has been mentioned that the distribution of urease in porous medium is very difficult to control and reliably measure. The final distribution of active enzymes in porous media caused by sorption, sedimentation, and interception is also difficult to quantically predict, which is dramatically dependent on the dominant process [45].

To investigate the effects of SSPS on the distribution of enzyme, a model analysis was conducted using a hybrid experimental-numerical approach.

4 Model analysis

4.1 Model assumptions and equations

It is interesting that the precipitation contents show a more homogenous distribution with a bit higher average value for S-3 samples compared to S-0 samples based on the analysis in the liquid environment test. Since the reaction rate of the whole SICP process with 3 g/L of SSPS is about 1.5 times of that without SSPS, it should result in a more uneven precipitation distribution for S-3 when compared with S-0 if similar enzyme distributions are assumed [21,27,43]. However, the actual precipitations distribute heterogeneously in S-0 but homogeneously in S-3. The possible mechanism is due to the different enzyme distribution in S-0 and S-3. In SICP without SSPS addition, the enzymes have been reported to form flocs with calcium cations and the large flocs might clog the pores near the inlet [28]. More enzymes will gather near the inlet and fewer enzymes can penetrate into deeper locations, resulting in heterogeneous enzyme distribution. Meanwhile, the gathered enzymes will produce more calcium carbonate within the same time and, together with the large flocs, extend the retention time of the substrates by reducing porosity and permeability. On the contrary, the enzymes might be more evenly distributed in S-3. The local variability related to these processes is hard to acquire through experiments. Hommel et al. [44] has been mentioned that the distribution of urease in porous medium is very difficult to control and reliably measure. The final distribution of active enzymes in porous media caused by sorption, sedimentation, and interception is also difficult to quantically predict, which is dramatically dependent on the dominant process [45].

1) Calcium precipitation is assumed to happen simultaneously with urea hydrolysis. Therefore, SICP process is expressed by a single reaction equation [44,46–49].

2) Once calcium precipitated with carbonate, the precipitation does not transport with liquid.

3) The nucleation and growth kinetics of calcium carbonate precipitation are not included.

4) The urea hydrolysis is assumed to be a first-order rate reaction with respect to urea concentration as suggested by Feder et al. [39], Hommel et al. [40], Lasisi and Akinremi [41], and Lei et al. [42].

5) The permeability changes of soil are assumed to be isotropic. The permeability changes of soil are assumed to be isotropic and follows Kozeny–Carman equation with no changes in the average diameter of soil particles as suggested by van Wijngaarden et al. [49].

6) The liquid and soil particles are considered non-compressible.

To get the calcium carbonate distribution in a porous media, the model equations should include the fluid flow, the transportation of substrates, reaction rate, the differential equations describing the changes in calcium carbonate precipitation and porosity, and finally the permeability relations with products following Qin et al. [38], Hommel et al. [44], Cunningham et al. [46], Minto et al. [48], van Wijngaarden et al. [49], Gai and Sánchez [50]. In this study, we build our model following the similar pattern as most researchers used. The reaction rates fitted with the liquid batch tests following the first-order kinetics in Subsection 3.1 were used when simulating different conditions. To be less redundant, some of the equations described in literature are presented in Table 1 and the simulation flowchart are shown in Fig. 6. The simulations were implemented by the finite element method in COMSOL Multiphysics.

4.2 Boundary conditions and initial values

A one-dimensional model was built to simulate the soil

Table 1 Some equations of the model

Procedure	Equations and parameter description
Calcium carbonate changes	$\frac{\partial C_{CaCO_3}}{\partial t} = R\theta M_{CaCO_3}$, (5) where $\partial C_{CaCO3}/\partial t$ is the change in calcium carbonate concentration in time, R is the reaction rate, θ is current porosity, M_{CaCO_3} is the molar weight of calcium carbonate, which is 100 g/mol.
Porosity changes	$\frac{\partial \theta}{\partial t} = \frac{\partial \left(C_{CaCO_3}\right)\theta}{\partial t}\frac{M_{CaCO_3}}{\rho_{CaCO_3}} = R\theta\frac{M_{CaCO_3}}{\rho_{CaCO_3}}$, (6) where ρ_{CaCO_3} is the density of calcium carbonate (calcite), which is 2710 kg/m^3.
Permeability changes	$\frac{K}{K_0} = \frac{(1-\theta_0)^2}{\theta_0^3}\frac{\theta^3}{(1-\theta)^2}$, (7) where K and K_0 are the current and initial intrinsic permeability, θ_0 is the initial porosity.
Fluid flow-Darcy's law	$u = -\frac{K}{\mu}\nabla p$, (8) where u is the Darcy's velocity, μ is viscosity of fluid, p is pressure.
Continuity equation	$\nabla \cdot (\rho u) = 0$, (9) ρ is the density of fluid.
Transport of solute substrates	$\frac{\partial}{\partial t}(\theta C) + \nabla \cdot (-\theta D \cdot \nabla C) + \nabla \cdot (Cu) = \theta R$, (10) C is the concentration of aqueous species and for every specie it can be written as C_i in which i represents different aqueous species. In SICP, i is urea, calcium, urease and ammonium. R represents the reaction rate for every aqueous specie and is determined by the reaction rate and the yield coefficient shown in hydrolysis Eq. (1). For urea, calcium, ammonium and urease, R equals to $-R$, $-R$, $2R$, and 0, respectively.

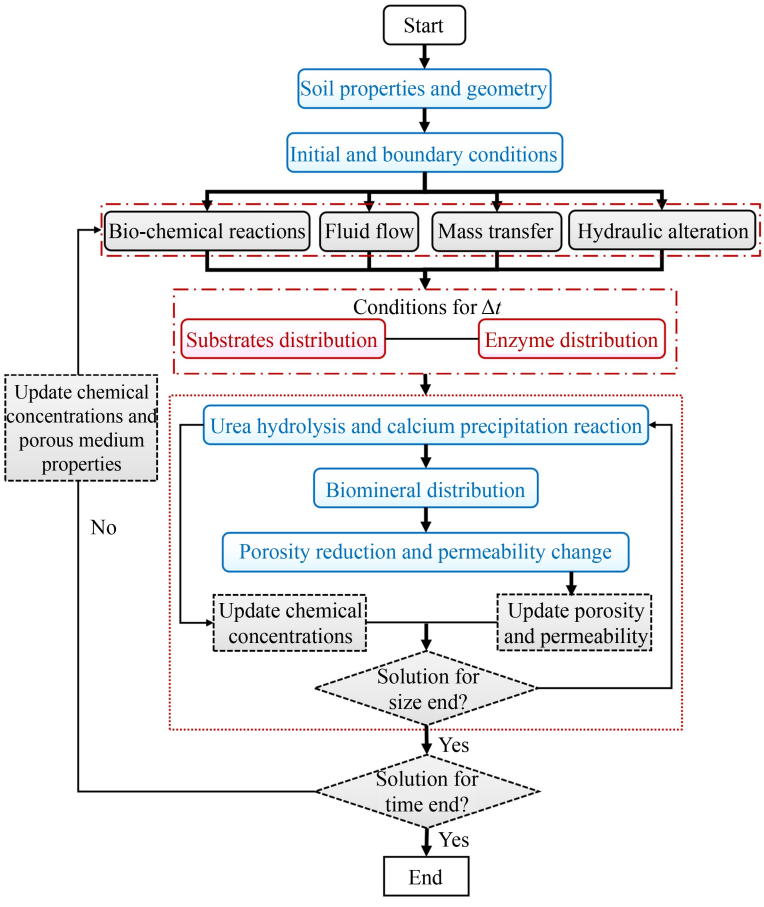

Fig. 6 Flowchart for simulation.

column tests done in this study. The length of the geometry is 0.1 m. The boundary conditions were set to simulate the situation that the specimens were flushed through by 90 mL of treatment solutions from top to bottom in about 12 min and then stay still for 30 h. Based on the dimensions of the specimen, a constant flow

boundary condition of 2.5×10^{-4} m/s was used for the top, and the flow lasted for 12 min as shown in Fig. 7. A zero-pressure boundary was applied to the bottom of the specimen. Reactions were implemented in the mass transportation process in porous medium. Constant urea and calcium concentrations of 0.4 mol/L were set as inflow boundary conditions for the top. An outflow boundary condition is applied to the bottom.

The initial concentration of urea, calcium and calcium carbonate were set to be zero. The initial porosity and intrinsic permeability of the porous medium are equal to the values of the soil specimen which are 0.425 and 2.528×10^{-11} m^2, respectively. During the flush, about 7–9 mL solution drained out from the specimen, which means that the pores within the specimen are almost fully filled with solutions. The remaining solutions were left in the soil for reaction as well, referring to the stagnant period. During the stagnant period, the distributions of enzymes as well as substrates were the same as those after flushing completed. Simulations were conducted by two steps: flushing and stagnant period. The flushing step lasts for 12 min (0.2 h), and the second step lasts for 30 h. Various parameters in the simulation were summarized in Table 2.

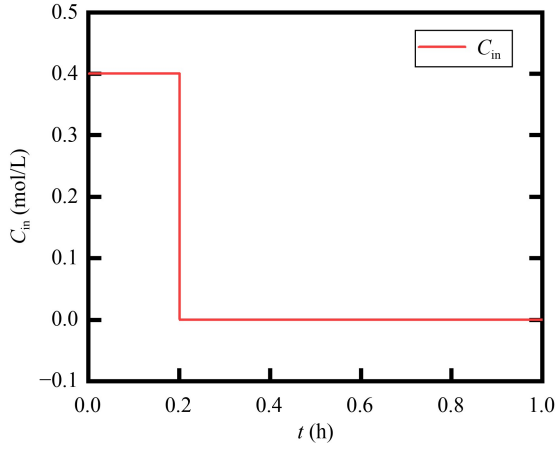

Fig. 7 Concentration boundary condition at the top of the specimen (Note: C_{in} represents the initial condition for both calcium and urea as equal molar of them were flushed into the specimens).

4.3 Calcium carbonate precipitation under different scenarios

In the first scenario, the enzymes were assumed as a diluted aqueous species for both S-0 and S-3 specimens. Normally the transportation of a diluted aqueous species is influenced by advection, diffusion, adsorption and/or desorption and reaction [44,46,48–51]. Pisani et al. [51] investigated the adsorption characteristics of urease enzyme on four soil components through a density functional theory and found that binding of amino acids (like urease enzyme in this study) to quartz is unfavorable. Since the soil used in this study is quartz sand, the transportation of enzymes in this study is assumed to be governed by convection and diffusion during the flushing step, after which the distributions of enzymes keep unchanged.

The molar concentration of urease is calculated by diving the mass concentration of extracted urease by the molar mass of urease when assuming that urease is the only protein in crude extracted enzyme from soybean. The molar mass of urease is about 480 kg/mol according to Polacco and Havir [52]. The resulting molar concentration of urease for the inflow boundary is about 0.00176 mol/m^3. It should be noted that the distribution of enzymes under this condition is the same for both S-0

Table 2 Values of the parameters in the simulation

Parameter	Value
Length of the soil column	$L = 0.1$ m
Inflow concentration during flow	$C_{in} = 0.4$ mol/L
Dynamic viscosity of fluids	$\mu = 1.15 \times 10^{-3}$ Pa·s
The first-order reaction rate coefficient for S-0 in the liquid batch test	$k_{S\text{-}0} = 0.0768$ h^{-1}
The enzyme concentration in the liquid batch tests and cementation solution used	$C_{et} = 1.76 \times 10^{-6}$ mol/L
Molecular mass of calcium carbonate	$M_{CaCO_3} = 100$ g/mol
Longitudinal dispersivity	$\alpha_L = 0.01$ m
Inflow velocity	$q_{in} = 2.5 \times 10^{-4}$ m/s
Initial porosity	$\theta_0 = 0.425$
Initial permeability	$K_0 = 2.528 \times 10^{-11}$ m^2
The first-order reaction rate coefficient for S-3 in the liquid batch test	$k_{S\text{-}3} = 0.1112$ h^{-1}
Molar mass of soybean urease	$M_{en} = 480 \times 10^3$ g/mol
Density of calcium carbonate (calcite)	$\rho_{CaCO_3} = 2710$ kg/m^3
Density of fluid	$\rho = 1000$ kg/m^3

and S-3 specimens as the related parameters are the same.

Figure 8 demonstrates the simulated results of urease at 0.2 h where X is the distance from the inlet port. It seems that urease is almost evenly distributed along the column. The simulated concentration of urea, calcium carbonate and porosity along the soil column at 0.2 h for S-0 and S-3 were shown in Figs. 9(a) and 9(b), respectively. Similar to the results of urease, the distribution of urea and porosity (θ) are the same for both S-0 and S-3, which are almost homogeneous along the column. It should be mentioned that, since the inflow condition, initial value and reaction rate of calcium are the same as urea, the distribution of calcium is the same as urea. For calcium carbonate concentration, it decreases with X for both cases and the largest values happen at the top. The decreasing trend of biominerals are the same for S-3 and S-0 but with different values. The largest calcium carbonate precipitation concentrations are 0.261 and 0.378 kg/m^3 for S-0 and S-3, respectively. Since the density of calcium carbonate is high and the precipitation amount is low, the resulting porosity changes are pretty tiny and seem unchanged along the soil column at the presented scale. But it should be noted that the porosity increases with the X for both cases.

The resulting distribution of urea, calcium and porosity after the flushing step were used as initial conditions for the stagnant step (from 0.2 to 30 h). There was no flow in this step, but the reaction was still going on. Reaction rates are set to be the same as that in the first step (flushing step, from 0 to 0.2 h). The calcium carbonate contents ($CaCO_3$ contents) during flushing and stagnant steps were added together and presented with respect to the dry mass percentage of soil as shown in Fig. 10. The measured data were presented in the same figure as well for comparison. For S-3, the simulated $CaCO_3$ contents are almost the same along the distance at about 0.86%, showing a homogenous distribution as presented in Fig. 10(a). The simulated results match the measured data well with the largest deviation of 3% at the bottom for S-3. Therefore, the simulation procedure and the boundary conditions are set correctly. However, for S-0, the simulated $CaCO_3$ contents demonstrate a homogeneous distribution while the measured $CaCO_3$ contents decrease with the distance and the lowest value happens at the bottom of the samples, as shown in Fig. 10(b). Compared to the simulated results, the measured $CaCO_3$ contents are higher at the top but lower at the middle and bottom of the specimens with the largest deviation of 56.7% at the bottom. It can be concluded that assuming enzyme transported like a diluted species for S-0 is not reasonable and the enzymes are not homogenously distributed in S-0, which indicates that 3 g/L SSPS have the function to improve the distribution of enzymes. For S-0, a second scenario is simulated where the distribution of enzyme is not homogeneous along the column in the following part.

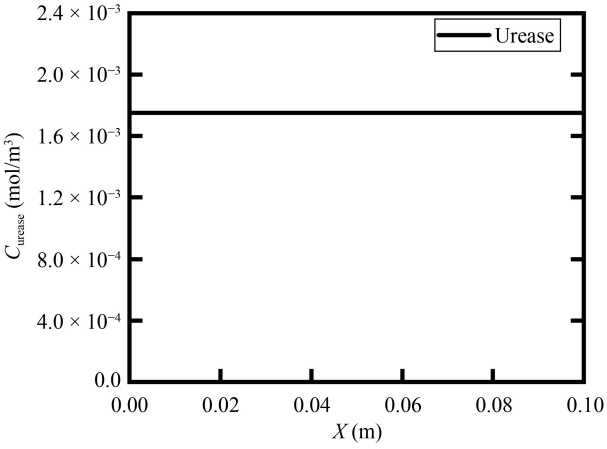

Fig. 8 The simulated distribution of urease which is assumed to be a diluted species.

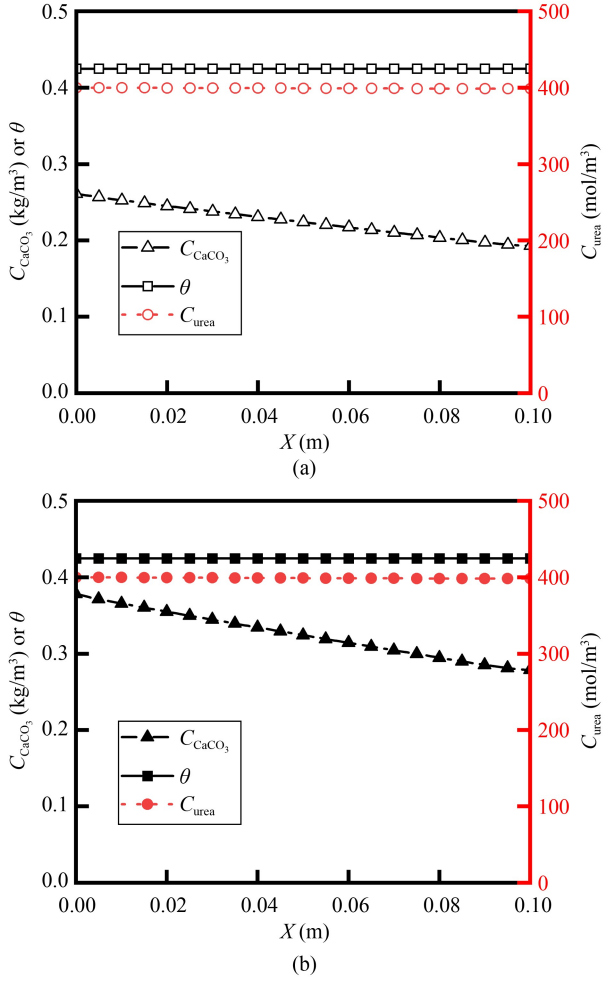

Fig. 9 The simulated distribution of urea, calcium carbonate and porosity along the column after flushing: (a) S-0; (b) S-3.

The high uncertainties of enzymes attachment measurements make it quite challenging to get the final distribution of the final active enzyme distribution in a porous media. However, the products (calcium carbonate

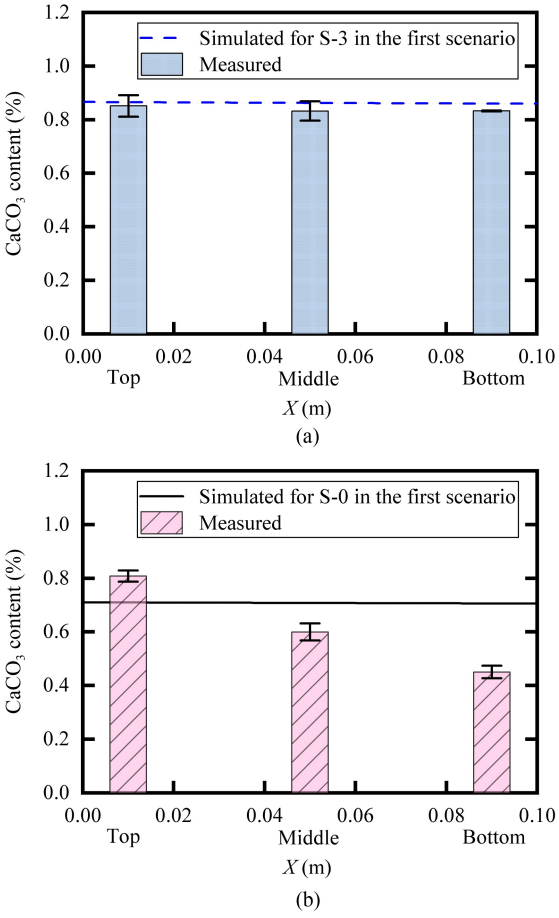

Fig. 10 Experimental and simulation results of calcium carbonate contents in the first scenario for: (a) S-3; (b) S-0 (Note: the first scenario referring to the case that enzyme is assumed as a diluted species).

in SICP) distribution is closely related to the distribution of enzymes [25]. Therefore, in many studies, the enzyme distribution was reasonably estimate based on the measured calcium carbonate distribution [31,44,47]. Thus, in the second scenario, the enzyme distribution in soil columns without SSPS were investigated based on the distribution of $CaCO_3$ contents using a hybrid experimental-numerical approach. According to the measured and simulated results in the first scenario, there should be more enzymes remaining at the top and less at the bottom after flushing so that with the same time more $CaCO_3$ are formed at the top. It is reasonable as enzyme can flocculate and form larger flocs which may get clogged at tiny spaces. Considering the confined space in the pores between soil grains and the low flow rate, more enzymes may gather near the inlet (top of the specimen in this study), resulting in a higher enzyme concentration. However, even though the distributions are different, the total amount of enzymes in the heterogenous scenario should not change so much compared to the homogeneous case. Based on the above analysis, in the following scenario, the distribution of enzymes is assumed to follow Eq. (11) to better describe the trends of the measured $CaCO_3$ contents and satisfy the mass balance of urease.

$$C_{ed} = \frac{a}{1+\left(\frac{X}{b}\right)^c} C_{et}, \tag{11}$$

where C_{ed} is the enzyme concentration at different locations, and X is the distance from the inlet. a, b, and c are the fitted constants. C_{et} is the total urease within the soil column, which is calculated to be 1.76×10^{-3} mol/m^3 according to the above analysis.

The values of a, b, and c are obtained based on two laws: well match with the measured data and the integrated urease content along the soil column are the same as the simulated results in the first scenario. Trail and errors are used to get simulation results. Figure 11(a) gives the urease distribution in the second scenario for S-0 which is modified based on the above-mentioned principles. The urease concentration at the top of the specimen is much higher than that in the homogeneous case while the middle and bottom are lower. At about 0.04 m, the modified urease concentration is the same as that in the first scenario. The resulting $CaCO_3$ contents simulated based on the modified urease distribution are

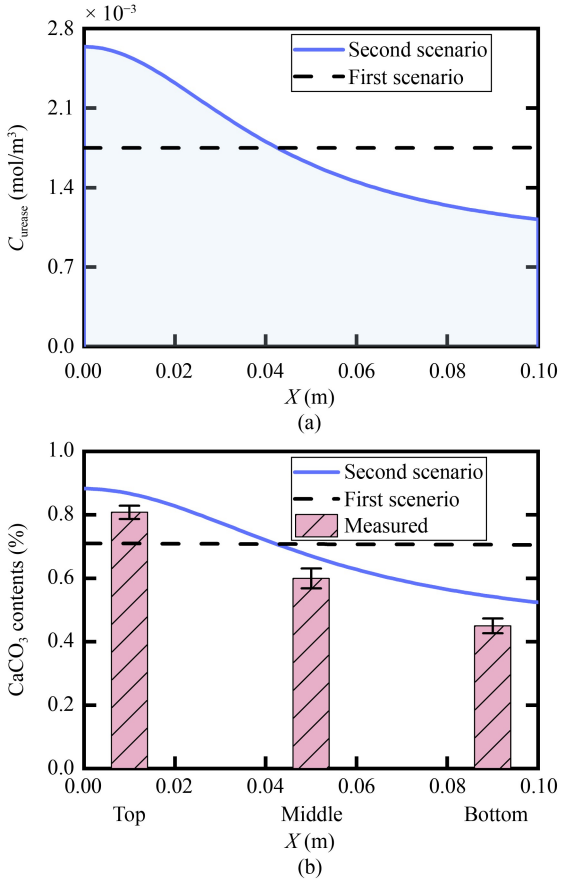

Fig. 11 (a) Modified urease distribution in the second scenario for S-0; (b) the resulting $CaCO_3$ contents for S-0.

shown in Fig. 11(b). It can be seen that the experimental developments of $CaCO_3$ contents are captured well by the simulation in this scenario. A large heterogeneity is demonstrated, where the highest value of about 0.883% is observed at the top and the lowest of 0.524% at the bottom. The simulated $CaCO_3$ contents are all a bit higher than the measured values for the top, middle and bottom of the specimen and the largest deviation is about 8.9% of the measured value. The difference of the simulated $CaCO_3$ contents between the top and the bottom are about 0.359%, which is almost the same as that in the measured data (0.357%). The same deviation and trend but different values indicates that the simulation is reasonable but there's some active enzymes loss in the total inputs for S-0 in the soil column experiment.

5 Discussion

In the specimens treated by ordinary all-in-one bio-cementation without any additions (S-0 in this study), more $CaCO_3$ biominerals were produced near the inlet either in the spraying or injection treatment methods even with only one time of treatment. Neupane et al. found that sever uneven urease distribution is the main reason [25]. Cheng et al. [27] pointed out that the existence of bio-flocculation was the main reason for uneven urease distribution. Beyond the flocculation of urease enzymes, the rapid formation of amorphous calcium carbonates (ACCs) presents another mechanism for pore clogging [53], particularly in high-supersaturation regimes. These bio-flocculation along with ACCs exist in a non-soluble state and will settle down by gravity and clog some pore space due to the large particle size. The clogging effect sometimes can promote a higher precipitation efficiency especially for medium with high and wide flow paths. Xiao et al. [54] found that there exists an appropriate injection rate for the sealing of rock fractures using the all-in-one continuous flow treatment, which balanced the excessive near-inlet clogging at low rates and reducing effects of depositions at high rates. The aggregation of catalytic media gathers at the inlet port of the specimen resulting in more biominerals at these places. The flocculated enzyme may have different transportation and activity characteristics, which will influence the enzyme distribution and consequently result in varied biomineral distribution. Yan et al. [28] reported that bio-flocs formed when the crude soybean urease was added to calcium solution. 0.01–0.02 mol/L of calcium can precipitate about 78% protein and reduce 53% activity for crude urease extracted from 80 g/L soybean. The reason why flocculation decreases the urease activity can be explained by the reduction in urease protein amounts and/or some active sites in the urease protein. The active sites are the places that help to reduce the energy activated for urea hydrolysis [55]. When the enzymes are flocculated, the proteins get intertwined and the active sites that are originally exposed to the solution are encapsulated in the flocs. These occluded active sites cannot function normally, which limits the accessibility to the substrates, thereby reducing catalytic efficiency [55]. Meanwhile, some researchers found that flocculation may change the structures of enzymes protein molecules, which is closely related to the activity of enzymes [56]. Distortion or alteration of the protein structure will affect its affinity and catalytic ability to substrates [57]. Enzymes flocculation before the introduction into soil will reduce the total active enzymes and/or site for the reaction inside the soil, resulting in fewer total biomineral contents within the same time as indicated by the difference between the measured and simulated results shown in Fig. 11(b). Though with enough time, the yield biomineral contents may also be less than that with higher activities depending on the values of activity and the decay trend of enzymes [58].

The distribution of urease is the outcome of enzyme transportation, which is influenced by flocculation and the resulting flocs transportation with flowing liquid, flocs clogging near the inlet or penetrating to longer distance with fast flow, adsorption and desorption to various soil mineral surfaces and so on. The transport of enzymes is also affected by the ion strength and the release of soil colloids from soil [59,60]. Guber et al. [59] pointed out that the enzyme's movement in an unrestricting volume of liquid did not necessarily imply the free movement in soil pores because of hydraulic discontinuity of water pathways in pores or polymeric restriction. Thus, it is quite difficult to get the distribution of enzyme through only numerical transportation simulation. However, the distribution of biominerals is the result of distribution of active enzymes. As a consequence, many researchers and models skip the complicated internal transportation process and measurements of urease but go straight to assume the resulting distribution of enzymes based on conceptual consideration. Homogeneous, exponentially decreased with increasing distance [44], exponentially increase with increasing distance [31] or a Gamma distribution [47] have been used to describe the ureolytic bacteria distribution along a column without the addition of calcium salts. However, the transportation of free enzymes in a porous media is different from microbes. Hoang et al. observed that microbes have a higher surficial attachment to the soil than the free enzyme in EICP [7]. For the scenario in which crude enzymes are transported with the presence of urea and calcium, the distribution pattern of enzymes is even less known. This study assumes crude soybean extracted enzyme distribution as presented by Eq. (10) gives a better description of the enzyme clogging at the upstream and

heterogenous biomineral distribution for all-in-one (enzyme mixed with reaction reagents) injection strategy.

The homogeneity of $CaCO_3$ distributed is largely improved by the addition of 3 g/L SSPS (S-3) as shown in the soil column test. As discussed above, normally two mechanisms are adopted to innervate the distribution of $CaCO_3$ in biologically treated medium: lowering the reaction rate and altering the urease distribution. From the liquid batch tests, it shows that 3 g/L addition increased the reaction rate by about 1.5 times. Thus, it is the urease distribution that S-3 improves resulting in a more homogeneous $CaCO_3$ distribution along the porous medium. The distribution of the urease along a soil column is difficult to obtain as mentioned by Hommel et al. [44], Gerlach [61], Cunningham et al. [62]. Meanwhile, as the proteins in the crude extracted soybean enzymes are not only urease but also other enzymes which may have different properties compared to urease. The possible varied adsorption and desorption of different proteins to the soil particles make it more difficult to quantify the urease amount at different locations. But we can have a rough picture of the urease distribution though measuring the protein amounts from the soil at different locations.

To get the effects of SSPS on protein distribution along the soil column, crude extracted soybean enzymes with or without 3 g/L SSPS were mixed with calcium solutions at 1:1 (resulting the same final calcium concentration and enzyme activity as in the soil column test) and then percolated into the specimens from the top to the bottom under the same boundary conditions as in the soil column tests. After that, the specimens were cut into five layers. Triple samples were taken out from different layers and mixed with deionized water at a ratio of 1:1 before being put into a shaker for 10 min. The mixtures were then centrifuged at 4000 rpm/min for 15 min. The protein amounts were determined by Bradford method in which proteins are dyed by Coomassie Brillian Blue and the optical density of dye-protein complex at 595 nm is linearly related to the concentration of protein.

The measured protein contents are shown in Fig. 12. The protein contents were presented as the total protein mass in milligrams per gram of dry soil. To better show the effects of SSPS on homogeneity of protein distribution, the measured data at different locations in both cases were normalized with respect to their individual values at the top. The results are also shown in Fig. 12. It shows that a dramatic decrease happens in protein contents for the second layer compared to the top before a gradual decrease with the distance from inlet. However, for the situation with 3 g/L SSPS addition, the difference of protein contents between the first two layers is much smaller. After the second layer, there're negligible changes in protein contents along the soil column though with only a bit decrease at the bottom.

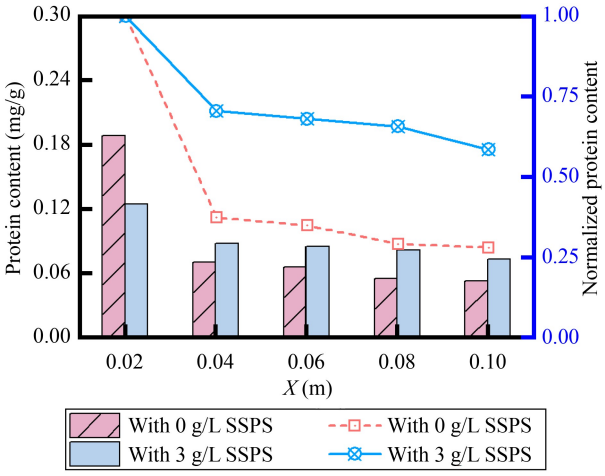

Fig. 12 Measured protein contents distribution with and without 3 g/L SSPS.

The development curve of protein contents along the column in the two cases indicates that 3 g/L of SSPS has positive effects on urease distribution in SICP treated soil. The positive effects of SSPS may be related to its stabilizing capacity of proteins. The stabilizing effects of SSPS help to avoid immediate flocculation of protein [63]. Asai et al. [63] presented that with only 0.3%, SSPS could inhibit intermolecular aggregation of milk protein, reducing the median diameter of protein from 10 to 3 μm. Phillips and William [64] mentioned that the anion groups in SSPS can bind to the surface of cationic ions or protein particles and the hydrophilic polysaccharide layers coated on the protein particles prevent aggregation by steric repulsion.

The lower protein contents at the bottom of the specimen without SSPS addition are consistent with the lower $CaCO_3$ contents compared to S-3 as shown in Fig. 5. Meanwhile, the protein contents at the top of the specimen without SSPS addition is higher than that with 3 g/L SSPS addition, which indirectly explains the higher calcium contents at the top of S-3 as shown in Fig. 5. It should be noted that the protein contents here are the total mass of all the proteins in crude extracted enzymes which include many other enzymes and proteins than urease. Meanwhile, the catalytic capacity of the urease is not positively linked to the mass of urease protein but the number of active protein/sites. As mentioned before, through the protein contents distribution, only a rough picture of urease distribution can be obtained. Therefore, it is still reasonable that the distribution of protein content does not fully follow the trends of $CaCO_3$ contents in soil column tests. To have a clear and comprehensive urease distribution, more advanced measuring techniques and analyzed methods are needed in the future.

X-Ray Diffraction (XRD) and scanning electron microscope (SEM) tests were conducted to analyze morphology and size of the precipitations. Figures 13(a)

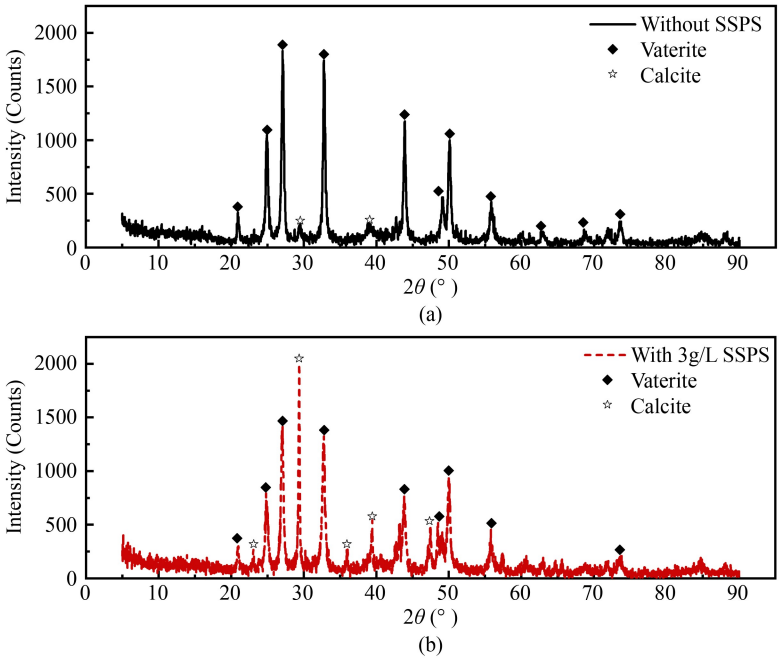

Fig. 13 XRD results of SICP treated soil: (a) without SSPS; (b) with 3 g/L SSPS.

and 13(b) show the XRD results of the treated soil with and without SSPS, respectively. It can be seen that the addition of 3 g/L SSPS increased the proportion of calcite in the precipitate compared to that without SSPS. This shift in polymorph is accompanied by a distinct change in crystal morphology and size, as observed by SEM as shown in Fig. 14. Figures 14(a)–14(c) illustrated the situations with SSPS while Figs. 14(d)–14(f) for samples without SSPS. It can be seen that with SSPS participation, the precipitate forms a denser, more coherent layer composed of numerous small, rhomboidal calcite crystals with an average size of approximately 700 nm. Meanwhile, many crystals, often associated with a smooth biofilm, are predominantly formed at the contacts between soil particles as shown in Figs. 14(a) and 14(b). In contrast, the precipitate formed without SSPS consists of larger, predominantly spherical particles ranging from 1.5–3.5 μm in size (Figs. 14(d)–14(f)). These results demonstrate that SSPS not only promotes the formation of the more stable calcite polymorph but also significantly refines crystal size and promotes a more integrated, matrix-like precipitation morphology that bridges soil particles.

From a sustainability perspective, SSPS, as a natural polysaccharide derived from soybean processing by-products (okara), embodies a waste-to-resource strategy that aligns with circular economic principles. Its use as a performance-enhancing additive in SICP not only improves the technical challenge of uneven precipitation but also reduces reliance on synthetic chemicals. This synergy between enhanced engineering efficacy and improved environmental profile makes the SSPS-augmented SICP a more sustainable and promising approach for field-scale applications.

6 Conclusions

This study investigated the role of SSPS in enhancing the uniformity of biologically induced calcium carbonate precipitation by soybean-urease, through a series of experiments and numerical analysis. One-time all-in-one SICP treatments, in which crude soybean urease, urea and calcium were mixed before introduction in soils, with and without SSPS addition were applied to soil columns. Meanwhile, both the enzymatic activity and transport behavior were analyzed. The results indicate that 3 g/L SSPS can serve as an effective additive in SICP, significantly improving the homogeneity of $CaCO_3$ distribution along the soil column. The largest deviation of the calcium carbonate contents which happens between the inlet and outlet for the tested soil and treatment conditions were reduced from 44% to 2% with SSPS addition. The uniformity enhancement was not attributed to a reduction in reaction rate, as often used in many other strategies, but rather to the improvement in the spatial distribution of urease, which was supported by numerical modeling and protein content measurements. Interestingly, the addition of SSPS also increased the overall reaction rate by 1.5 times, suggesting a dual benefit of reaction acceleration and homogenization. The underlying mechanism may lie in the protein-stabilizing effect of SSPS, which mitigates flocculation-induced clogging near the inlet and protects active catalytic sites, thus maintaining enzyme mobility and accessibility. Simulation results further confirmed that non-uniform enzyme distribution without SSPS could lead to severe heterogeneity in biomineral formation, while the inclusion of SSPS leads to a more even spatial profile of

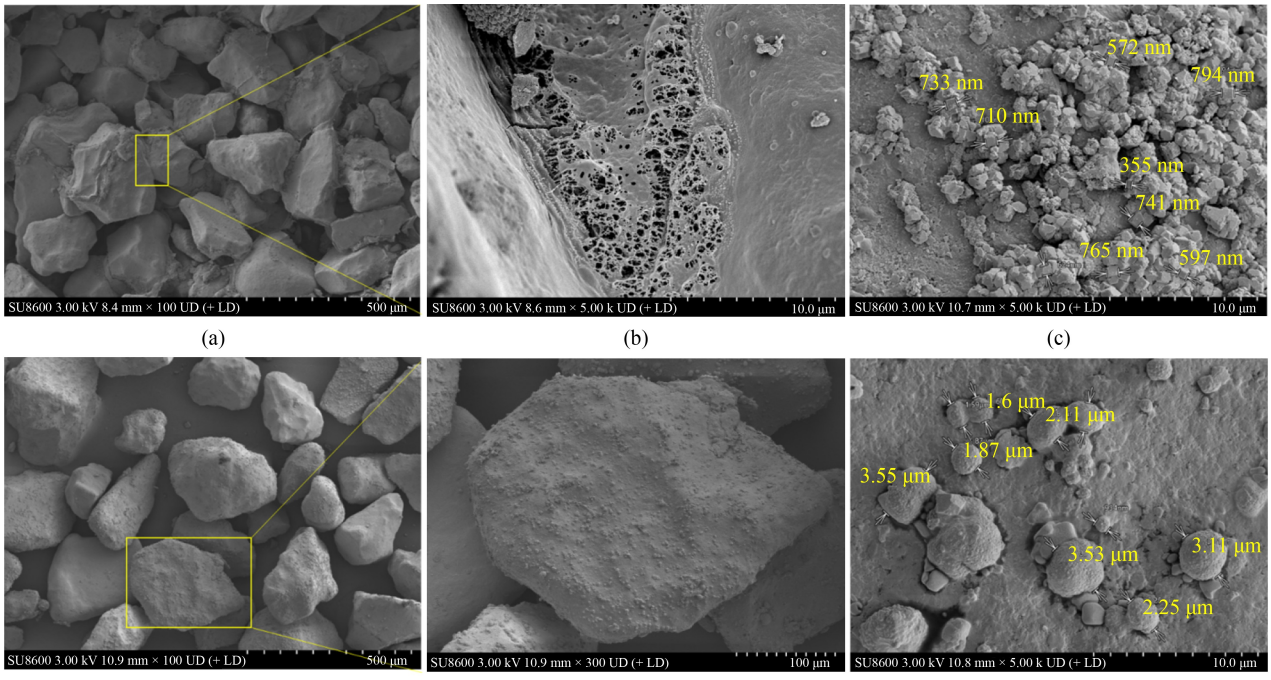

Fig. 14 SEM of treated soils: (a) panorama of the micromorphology of soils treated with SICP with 3 g/L SSPS; (b) local magnification of (a) showing biofilm between grains; (c) size of biominerals in soils induced by SICP with 3 g/L SSPS; (d) panorama of the micromorphology of soils treated with SICP without SSPS; (e) local magnificent of (d); (f) size of biominerals in soils induced by SICP without SSPS.

precipitation, closely matching experimental data. Overall, this work demonstrates that SSPS is a promising natural additive to enhance SICP treatment uniformity without sacrificing reaction efficiency. The findings provide a practical pathway to improve the field applicability of SICP in geotechnical and environmental engineering.

Acknowledgements This study was supported by the National Natural Science Foundation of China (Grant Nos. 52208357 and 52408359), Hebei Natural Science Foundation (No. E2023201036) and Technology Project of Hebei Education Department (No. BJK2024175). The authors would also like to acknowledge the support by the HBU Innovation Team for Multi-disaster Prevention in Transportation Geotechnics (No. IT2023C04).

Competing interests The authors declare that they have no competing interests.

References

1. Ahmadzadeh E, Samadianfard S, Xiao Y, Toufigh V. Feasibility of micro-organisms in soil bioremediation and dust control. Biogeotechnics, 2024, 2(3): 100085
2. He J, Liu Y, Liu L, Yan B, Li L, Meng H, Hang L, Qi Y, Wu M, Gao Y. Recent development on optimization of bio-cementation for soil stabilization and wind erosion control. Biogeotechnics, 2023, 1(2): 100022
3. Liu Y, Gao Y, He J, Zhou Y, Geng W. An experimental investigation of wind erosion resistance of desert sand cemented by soybean-urease induced carbonate precipitation. Geoderma, 2023, 429: 116231
4. Meng H, Gao Y, He J, Qi Y, Hang L. Microbially induced carbonate precipitation for wind erosion control of desert soil: Field-scale tests. Geoderma, 2021, 383: 114723
5. Xiao Y, He X, Zaman M, Ma G, Zhao C. Review of strength improvements of biocemented soils. International Journal of Geomechanics, 2022, 22(11): 03122001
6. Gao Y, He J, Tang X, Chu J. Calcium carbonate precipitation catalyzed by soybean urease as an improvement method for fine-grained soil. Soils and Foundations, 2019, 59(5): 1631–1637
7. Hoang T, Alleman J, Cetin B, Ikuma K, Choi S G. Sand and silty-sand soil stabilization using bacterial enzyme-induced calcite precipitation (BEICP). Canadian Geotechnical Journal, 2019, 56(6): 808–822
8. Xiao Y, Zhang Z, Stuedlein A W, Evans T M. Liquefaction modeling for biocemented calcareous sand. Journal of Geotechnical and Geoenvironmental Engineering, 2021, 147(12): 04021149
9. Almajed A, Khodadadi Tirkolaei H, Kavazanjian E Jr. Baseline investigation on enzyme-induced calcium carbonate precipitation. Journal of Geotechnical and Geoenvironmental Engineering, 2018, 144(11): 04018081
10. Almajed A, Tirkolaei H K, Kavazanjian E Jr, Hamdan N. Enzyme induced biocementated sand with high strength at low carbonate content. Scientific Reports, 2019, 9(1): 1135
11. Martin K, Tirkolaei H K, Kavazanjian E. Enhancing the strength of granular material with a modified enzyme-induced carbonate precipitation (EICP) treatment solution. Construction & Building

Materials, 2021, 271: 121529
12. Fu T, Saracho A C, Haigh S K. Microbially induced carbonate precipitation (MICP) for soil strengthening: A comprehensive review. Biogeotechnics, 2023, 1(1): 100002
13. He J, Gao Y, Gu Z, Chu J, Wang L. Characterization of crude bacterial urease for $CaCO_3$ precipitation and cementation of silty sand. Journal of Materials in Civil Engineering, 2020, 32(5): 04020071
14. Xiao Y, He X, Stuedlein A W, Chu J, Matthew Evans T, van Paassen L A. Crystal growth of MICP through microfluidic chip tests. Journal of Geotechnical and Geoenvironmental Engineering, 2022, 148(5): 06022002
15. Zhang J, Xiao Y, Cui H, He X, Liu H. Dancing with crystals: Bacterial functions and interactions in biomineralization. Biogeotechnics, 2024, 2(3): 100084
16. Zhao C, Xiao Y, He X, Liu H, Liu Y, Chu J. Influence of injection methods on bio-mediated precipitation of carbonates in fracture-mimicking microfluidic chip. Geotechnique, 2025, 75(2): 153–165
17. Chen Y, Gao Y, Guo H. Bio-improved hydraulic properties of sand treated by soybean urease induced carbonate precipitation and its application. Part 2: Sand-geotextile capillary barrier effect. Transportation Geotechnics, 2021, 27: 100484
18. Hamdan N, Kavazanjian E Jr. Enzyme-induced carbonate mineral precipitation for fugitive dust control. Geotechnique, 2016, 66(7): 546–555
19. Zhang J, Yin Y, Shi W, Bian H, Shi L, Wu L, Han Z, Zheng J, He X. Strength and uniformity of EICP-treated sand under multi-factor coupling effects. Biogeotechnics, 2023, 1(1): 100007
20. Maleki M, Ebrahimi S, Asadzadeh F, Emami Tabrizi M. Performance of microbial-induced carbonate precipitation on wind erosion control of sandy soil. International Journal of Environmental Science and Technology, 2016, 13(3): 937–944
21. Cui M, Lai H, Hoang T, Chu J. One-phase-low-pH enzyme induced carbonate precipitation (EICP) method for soil improvement. Acta Geotechnica, 2021, 16(2): 481–489
22. DeJong J T, Fritzges M B, Nüsslein K. Microbially induced cementation to control sand response to undrained shear. Journal of Geotechnical and Geoenvironmental Engineering, 2006, 132(11): 1381–1392
23. Nafisi A, Safavizadeh S, Montoya B M. Influence of microbe and enzyme-induced treatments on cemented sand shear response. Journal of Geotechnical and Geoenvironmental Engineering, 2019, 145(9): 06019008
24. Wang Y, Liu H, Zhang Z, Xiao P, He X, Xiao Y. Study on low-strength biocemented sands using a temperature-controlled MICP (microbially induced calcite precipitation) method. In: Khabbaz H, Youn H, Bouassida M, eds. New Prospects in Geotechnical Engineering Aspects of Civil Infrastructures—GeoChina 2018—Sustainable Civil Infrastructures. Cham: Springer, 2019, 15–26
25. Neupane D, Yasuhara H, Kinoshita N, Putra H. Distribution of grout material within 1-m sand column *in situ* calcite precipitation technique. Soils and Foundations, 2015, 55(6): 1512–1518
26. Zhao C, Xiao Y, Liu H, Chu J. Effects of urease and cementing solution concentrations on micro-scale enzymatic mineralisation characteristics. Geotechnique, 2025, 75(6): 732–746
27. Cheng L, Shahin M A, Chu J. Soil bio-cementation using a new one-phase low-pH injection method. Acta Geotechnica, 2019, 14(3): 615–626
28. Yan B, Zhou Y, Li C, Shu S, Gao Y. Modified SICP method to mitigate the effect of bio-clogging by excess protein from soybean crude urease extracts for biocementation process. Acta Geotechnica, 2023, 18(9): 5047–5062
29. Mi H, Zhang Y, Zhao Y, Li J, Chen J, Li X. Cryoprotective effect of soluble soybean polysaccharides and enzymatic hydrolysates on the myofibrillar protein of Nemipterus virgatus surimi. Food Chemistry, 2024, 446: 138903
30. Song H, Zhang Z, Li Y, Zhang Y, Yang L, Wang S, He Y, Liu J, Zhu D, Liu H. Effects of different enzyme extraction methods on the properties and prebiotic activity of soybean hull polysaccharides. Heliyon, 2022, 8(11): e11053
31. Barkouki T H, Martinez B C, Mortensen B M, Weathers T S, De Jong J D, Ginn T R, Spycher N F, Smith R W, Fujita Y. Forward and inverse bio-Geochemical modeling of microbially induced calcite precipitation in half-meter column experiments. Transport in Porous Media, 2011, 90(1): 23–39
32. Whiffin V S. Microbial $CaCO_3$ precipitation for the production of biocement. Dissertation for the Doctoral Degree. Perth: Murdoch University, 2004
33. ISO 6058. Water Quality-Determination of Calcium Content-EDTA Titrimetric Method. Geneva: International Organization for Standardization, 1984
34. Gao Y, Wang L, He J, Ren J, Gao Y. Denitrification-based MICP for cementation of soil: Treatment process and mechanical performance. Acta Geotechnica, 2022, 17(9): 3799–3815
35. ASTM. Standard Practice for Classification of Soils for Engineering Purposes (Unified Soil Classification System), ASTM D2487-00. West Conshohocken, PA: ASTM, 2000
36. Kim D H, Mahabadi N, Jang J, van Paassen L A. Assessing the kinetics and pore-scale characteristics of biological calcium carbonate precipitation in porous media using a microfluidic chip experiment. Water Resources Research, 2020, 56(2): e2019WR025420
37. Van Paassen L A. Biogrout, ground improvement by microbial induced carbonate precipitation. Dissertation for the Doctoral Degree. Delft: Delft University of Technology, 2009
38. Qin C Z, Hassanizadeh S M, Ebigbo A. Pore-scale network modeling of microbially induced calcium carbonate precipitation: Insight into scale dependence of biogeochemical reaction rates. Water Resources Research, 2016, 52(11): 8794–8810
39. Feder M J, Akyel A, Morasko V J, Gerlach R, Phillips A J. Temperature-dependent inactivation and catalysis rates of plant-based ureases for engineered biomineralization. Engineering Reports, 2021, 3(2): e12299
40. Hommel J, Akyel A, Frieling Z, Phillips A J, Gerlach R, Cunningham A B, Class H. A numerical model for enzymatically induced calcium carbonate precipitation. Applied Sciences, 2020, 10(13): 4538
41. Lasisi A A, Akinremi O O. Kinetics and thermodynamics of urea hydrolysis in the presence of urease and nitrification inhibitors. Canadian Journal of Soil Science, 2021, 101(2): 192–202
42. Lei T, Gu Q, Guo X, Ma J, Zhang Y, Sun X. Urease activity and

urea hydrolysis rate under coupling effects of moisture content, temperature, and nitrogen application rate. International Journal of Agricultural and Biological Engineering, 2018, 11(2): 132–138

43. van Wijngaarden W K, van Paassen L A, Vermolen F J, van Meurs G A M, Vuik C. A reactive transport model for biogrout compared to experimental data. Transport in Porous Media, 2016, 111(3): 627–648
44. Hommel J, Lauchnor E, Gerlach R, Cunningham A B, Ebigbo A, Helmig R, Class H. Investigating the influence of the initial biomass distribution and injection strategies on biofilm-mediated calcite precipitation in porous media. Transport in Porous Media, 2016, 114(2): 557–579
45. Tufenkji, N. Modeling microbial transport in porous media: Traditional approaches and recent developments. Advances in Water Resources, 2007, 30(6-7): 1455–1469.
46. Cunningham A B, Class H, Ebigbo A, Gerlach R, Phillips A J, Hommel J. Field-scale modeling of microbially induced calcite precipitation. Computational Geosciences, 2019, 23(2): 399–414
47. Martinez B C, DeJong J T, Ginn T R. Bio-geochemical reactive transport modeling of microbial induced calcite precipitation to predict the treatment of sand in one-dimensional flow. Computers and Geotechnics, 2014, 58: 1–13
48. Minto J M, Lunn R J, El Mountassir G. Development of a reactive transport model for field-scale simulation of microbially induced carbonate precipitation. Water Resources Research, 2019, 55(8): 7229–7245
49. van Wijngaarden W K, Vermolen F J, van Meurs G A M, Vuik C. Modelling biogrout: A new ground improvement method based on microbial-induced carbonate precipitation. Transport in Porous Media, 2011, 87(2): 397–420
50. Gai X, Sánchez M. An elastoplastic mechanical constitutive model for microbially mediated cemented soils. Acta Geotechnica, 2019, 14(3): 709–726
51. Pisani W A, Jenness G R, Schutt T C, Larson S L, Shukla M K. Preferential adsorption of prominent amino acids in the urease enzyme of sporosarcina pasteurii on arid soil components: A periodic DFT study. Langmuir, 2022, 38(44): 13414–13428
52. Polacco J C, Havir E A. Comparisons of soybean urease isolated from seed and tissue culture. Journal of Biological Chemistry, 1979, 254(5): 1707–1715
53. Xiao Y, Zhao C, Cui H, Chen Y, Wu B, Liu H. Microscale insights into enzyme-induced carbonate precipitation in rock-based microfluidic chips. Geotechnique, 2025, 75(7): 846–857
54. Xiao Y, Zhao C, Fang Q, He X, Chu J, Liu H. Visualizing enzyme-induced mineralization in fractures. Journal of Rock Mechanics and Geotechnical Engineering, 2025
55. Robinson P K. Enzymes: Principles and biotechnological applications. Essays in Biochemistry, 2015, 59: 1–41
56. Mazzei L, Cianci M, Benini S, Ciurli S. The structure of the elusive urease–urea complex unveils the mechanism of a paradigmatic nickel-dependent enzyme. Angewandte Chemie International Edition, 2019, 58(22): 7415–7419
57. Li Y, Chen Z, Li H, Yao Q, Wei Y, Wang X, Wang N, Cao X, Zheng M, Lv J, et al. Improving dewaterability of sewage sludge by inoculating acidified sludge and Fe^{2+}: Performance and mechanisms. Process Safety and Environmental Protection, 2022, 158: 210–220
58. Javadi N, Khodadadi Tirkolaei H, Hamdan N, Kavazanjian E J. Longevity of raw and lyophilized crude urease extracts. Sustainable Chemistry, 2021, 2(2): 325–334
59. Guber A, Blagodatskaya E, Kravchenko A. Are enzymes transported in soils by water fluxes? Soil Biology & Biochemistry, 2022, 168: 108633
60. Sheng Y, Dong H, Coffin E, Myrold D, Kleber M. The important role of enzyme adsorbing capacity of soil minerals in regulating β-glucosidase activity. Geophysical Research Letters, 2022, 49(6): e2021GL097556
61. Gerlach R. Transport and activity of dissimilatory metal-reducing bacteria in porous media for the remediation of heavy metals and chlorinated hydrocarbons. Dissertation for the Doctoral Degree. Bozeman, MT: Montana State University, 2001
62. Cunningham A B, Sharp R R, Caccavo F Jr, Gerlach R. Effects of starvation on bacterial transport through porous media. Advances in Water Resources, 2007, 30(6–7): 1583–1592
63. Katsuyoshi N, Etsushiro D, eds. Food Hydrocolloids. New York, NY: Springer, 1993, 151–156
64. Phillips G O, Williams P A. Handbook of Hydrocolloids. 2nd ed. Boca Raton, FL: Woodhead Publishing, 2009